

## The effects of room temperature aging upon the magnetic properties of Ba-hexaferrite films grown on 6H-SiC substrates

Z. Chen,<sup>1,a)</sup> Zhuhua Cai,<sup>2</sup> Aria Yang,<sup>1</sup> Katherine S. Ziemer,<sup>2</sup> Carmine Vittoria,<sup>1</sup> and V. G. Harris<sup>1</sup>

<sup>1</sup>*Department of Electrical and Computer Engineering, Northeastern University, Boston, Massachusetts 02115, USA*

<sup>2</sup>*Department of Chemical Engineering, Northeastern University, Boston, Massachusetts 02115, USA*

(Presented on 7 November 2007; received 13 September 2007; accepted 12 December 2007; published online 21 March 2008)

The successes of making acceptable magnetic properties BaM films by different techniques based on pulsed laser deposition were reported in the past years. The key was to introduce a proper buffer layer to promote two dimensional growths on these semiconductor material substrates. After years, we go back to characterize these samples made by different processings. The purpose of this experiment is to explore the role of the buffer layers especially with the time dependence and thus demonstrate our film suitable for the potential future application. These samples are characterized by scanning electron microscopy, x-ray diffraction, and vibrating sample magnetometry comparing to characteristics of the as deposited films. © 2008 American Institute of Physics.

[DOI: [10.1063/1.2839327](https://doi.org/10.1063/1.2839327)]

### INTRODUCTION

The integration of microwave magnetic devices (e.g., isolators, circulators, phase shifters, etc.) with semiconductor integrated circuits has been a long standing goal in the microwave integrated circuit industry.<sup>1</sup> Previous attempts to grow high quality ferrites on Si and GaAs substrates have failed due to interface alloying and chemical decomposition, respectively. The principle challenge is the high temperatures required for the growth of high quality, low loss ferrites. These high temperatures lead to the degradation of most semiconductor materials. Recently, Chen *et al.*<sup>2,3</sup> demonstrated the growth of high quality epitaxial Ba-hexaferrite films on 6H-SiC substrates. 6H-SiC (0001) was chosen as the substrate because it has the same hexagonal crystal structure as barium ferrite (BaFe<sub>12</sub>O<sub>19</sub>, BaM) with a lattice mismatch of 4.38%. Additionally, its thermal and chemical stability are suitable for the high temperature processing required by ferrites. One aspect that is not commonly explored is the time stability of the ferrites and their interaction with the substrate. For practical applications, the film's stability of the physical and mechanical properties over time is essential. In order to evaluate the BaM film quality as a function of room temperature aging, we returned to the original samples grown more than 18 months ago. There, we observed changes in their structural and magnetic properties that were unexpected and in some cases remarkable. Films studied here include those grown on bare SiC as well as some with MgO interwoven buffer layers.<sup>3</sup> MgO has proven to be a suitable buffer layer due to its tolerable mismatch to the BaM hexaferrite ~1.3%, and its mismatch to 6H-SiC, ~3.23%.<sup>4,5</sup>

### EXPERIMENTS

The samples studied here were all prepared by conventional pulsed laser deposition (PLD) from a single homogeneous pure phase magnetoplumbite target approximately 18 months ago from the time of this submission. The substrate was a single crystal 6H-SiC (0001) procured from Cree, Inc. One variable in the processing is the surface preparation of the SiC substrate prior to deposition. Based on previous work,<sup>2,3</sup> the optimal substrate surface preparation included boiling in H<sub>2</sub>SO<sub>4</sub>+H<sub>2</sub>O<sub>2</sub> and rinses in dilute HF and HCl+H<sub>2</sub>O<sub>2</sub> solutions which was referred as wet cleaning. Other surface preparation include a dry plasma etch followed by hydrogen termination, which was referred as dry cleaning. The deposition was carried out by PLD with a KrF excimer laser operating at a wavelength of 248 nm. For the first generation samples, represented by G1-dry and G1-wet, the laser was operating at an energy level of 200 mJ/pulse, the deposition oxygen pressure and substrate temperature was ~300 mTorr and 800 °C, respectively. The processing conditions for the second generation samples, represented by G2, were quite different. It was grown at 925 °C and 20 mTorr of oxygen pressure using 250 mJ/laser pulse. G2 sample processing was the optimized condition for BaM growth on 6H-SiC substrate.<sup>3,5</sup> Furthermore, G1 samples were prepared by depositing BaM directly on SiC substrate while G2 sample adopted the use of a thin graduated MgO multilayer in the early stages of film growth. The multilayer consists of MgO layers interwoven with BaM layers. For example, [MgO(A)/BaM(B)]<sub>n</sub>, where A is the thickness of the MgO layer, B is the thickness of the BaM layer, and n is the number of repeats. The layer thickness is controlled by the number of laser shots incident upon each target. The first period is the thickest at A=80 shots and B=150 shots. Subsequent repeats have the thickness of MgO layer (A) reduced by ten shots. After nine periods, the MgO growth was

<sup>a)</sup>Electronic mail: [zchen@ece.neu.edu](mailto:zchen@ece.neu.edu).

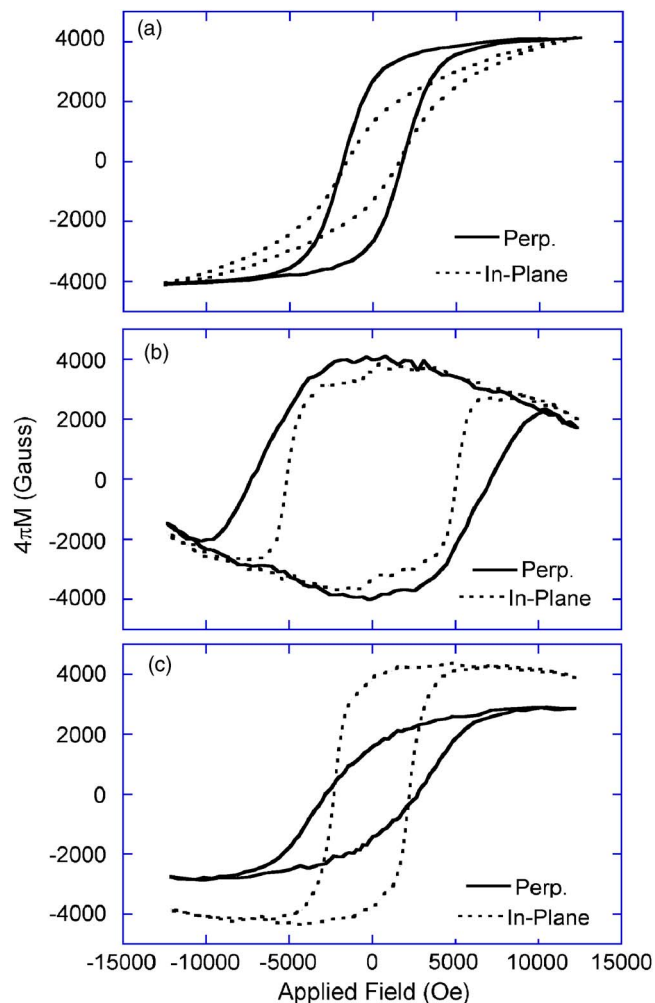


FIG. 1. (Color online) The hysteresis loops of (a) the generation I sample prepared at 300 mTorr, which represents the vibrating sample magnetometer measurement of samples G1-wet and G1-dry as grown. (b) sample G1-wet recently measured after the samples aged 18 months. (c) Sample G1-dry recently measured after the samples aged 18 months.

stopped and a thick BaM layer ( $\sim 500$  nm) was then grown. A single laser shot provides  $\sim 0.01$  nm of MgO and BaM, respectively. In this growth scheme the interfacial region of the film exists as a layered, and possibly alloyed, structure. The purpose is to gradually reduce the strain at the interface. Compared with G1 samples, G2 films grown via this approach were found to have better orientation and much less interface diffusion between the deposited BaM film and SiC substrate. As a result, the ferromagnetic resonance linewidth of G2 was reduced to 500 Oe from 1200 Oe.<sup>3</sup>

## RESULTS AND DISCUSSIONS

The film aging effect was first noticed by collecting hysteresis loops by vibrating sample magnetometry of older films. In Fig. 1(a), we illustrate the as-grown hysteresis loops of the G1 film grown under 300 mTorr oxygen pressures. These data represent a benchmark for changes observed in the older films designated G1-wet and G1-dry. In these data, one sees a uniaxial anisotropy with the magnetic easy axis aligned out of the film plane. The anisotropy field is difficult to ascertain since the hard axis loop does not saturate but we estimate the  $H_a$  to be 13.5–14.5 kOe. These values are sig-

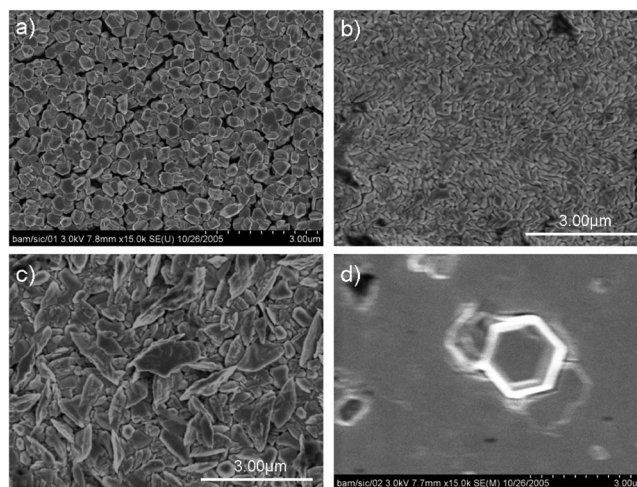


FIG. 2. The SEM images of (a) the G1 sample prepared at 300 mTorr, which is representative for samples G1-wet and G1-dry as grown, (b) sample G1-wet recently scanned, (c) sample G1-dry recently scanned, and (d) sample G2 as grown.

nificantly less than single crystal BaM values typically quoted at 17 kOe.<sup>6</sup> The reason for this discrepancy is the diffusion of Si into the film likely reducing the anisotropy by Si cation substitution. Figure 2(a) is a scanning electron microscopy (SEM) micrograph of the BaM film morphology in the as-grown state. One sees hexagonal grains of approximately  $0.3\text{--}0.5$   $\mu\text{m}$  in diameter arranged with their basal planes parallel to the film plane. Figure 2(d) is a similar micrograph taken of a film grown at lower pressures and higher temperature with an MgO interwoven buffer layer. Clearly, this is a film of superior quality in which larger hexagonal grains ( $1.5\text{--}2$   $\mu\text{m}$  in diameters) oriented similarly with their basal planes parallel to the film plane. We now consider the aged films.

In Fig. 1(b), similar hysteresis data are shown from G1-wet film collected after 18 months of room temperature aging in a desiccator. Clearly, the hysteresis loop shape has dramatically changed. A significant increase is seen in the coercivity from 1600 to 5000 Oe, and the preference for out of plane anisotropy is reduced to nearly an isotropic state. Surprisingly, the saturation magnetization remains largely unchanged near 4000 G. Figure 2(b) is a SEM micrograph of this film's microstructure. The hexagonal platelets seen in Fig. 2(a) have been replaced with a herringbone arrangement of acicular particles in which the long axis is of the same magnitude as the platelets of Fig. 2(a) with the short axis about  $0.13$   $\mu\text{m}$ . It may be that these particles are in fact the hexagonal platelets now arranged with the basal plane orthogonal to the film plane.

In Fig. 1(c), hysteresis data are presented for G1-dry sample. In this case, the SiC substrate was wet etched followed by a dry plasma etch and hydrogen termination. The hysteresis loops bare resemblance to the original film data collected 18 months ago in that the saturation magnetization remains near 4000 G, the coercive fields have increased from 1600 to 1750 Oe. However, what is remarkable is that we now observe a uniaxial anisotropy with the magnetic easy axis aligned in the film plane. This in fact is opposite to that of the original film.

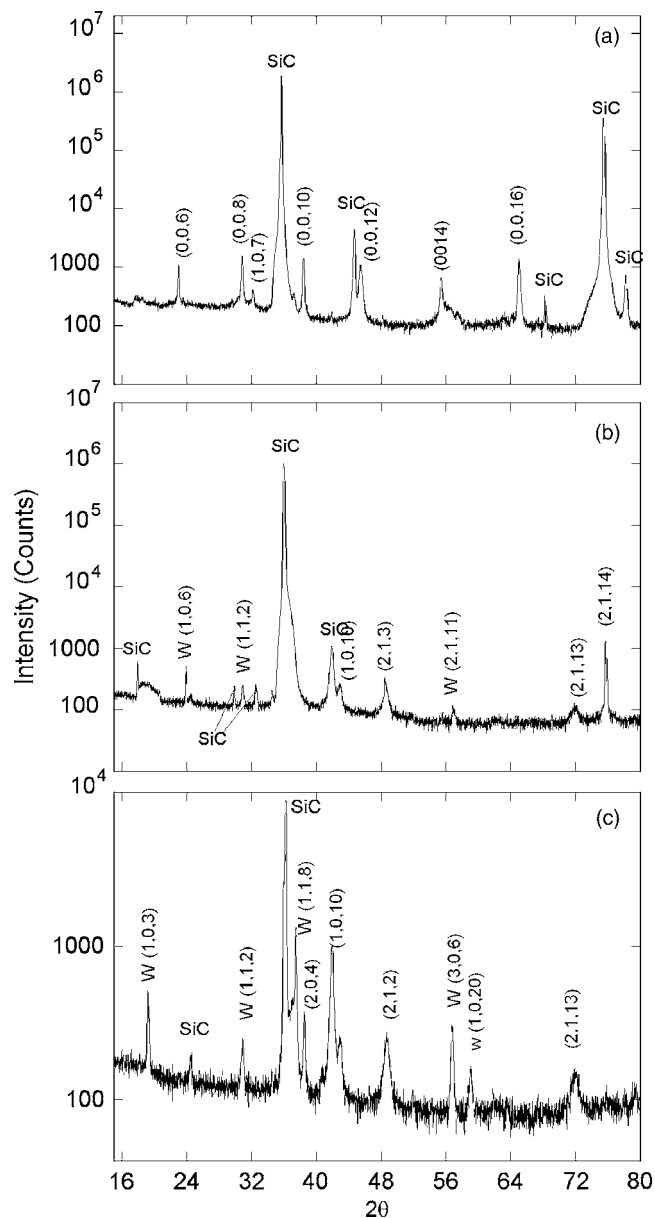


FIG. 3. The XRD spectrum of (a) G1 sample prepared at 300 mTorr which represented sample G1-wet and G1-dry as grown, (b) sample G1-wet recently collected, and (c) sample G1-dry recently collected. “W” in the peaks index represents the *W*-type  $\text{BaFe}_{18}\text{O}_{27}$ .

G1-dry film morphology is depicted in Fig. 2(c). In comparing this morphology to that of Fig. 2(a), we see an increase in acicular particle size to  $1.5\ \mu\text{m}$  (long axis) and  $0.3\text{--}0.5\ \mu\text{m}$  (short axis). The grain size appears to be broad and perhaps bimodal. Once again the morphology and magnetization data are consistent with hexagonal platelets arranged with their basal planes orthogonal to the film plane.

X-ray diffraction data as  $\theta$ - $2\theta$  scans using  $\text{Cu K}\alpha$  radiation are presented in Figs. 3(a)–3(c). In Fig. 3(a), the x-ray

diffraction (XRD) pattern is for the as-grown sample in which all diffraction peaks are indexed to the BaM hexaferrite phase. The profile is dominated by  $(0,0,2n)$  diffraction peaks verifying the strong crystal texture present in the film. Figure 3(b) is corresponding data for G1-wet film sample. In these data, all peaks are indexed to both the *M*-type and a secondary *W*-type ( $\text{BaFe}_{18}\text{O}_{27}$ ) hexaferrite phases. The appearance of the *W*-type ferrite phase (as weak peaks) is surprising since no previous reports have alluded to the time evolution of *M*-type to *W*-type hexaferrite. This trend toward the transformation of *M*-type to *W*-type hexaferrite is more pronounced in Fig. 3(c) (G1-dry) where the *W* ferrite peaks are dominant.

In review of these data and trends, it is unclear as to the dominant mechanism that gives rise to these dramatic changes in the magnetic, structural, and morphological properties of these films. It is likely that the strain existing at the film-substrate interface is the driving force behind these changes. If the strain energy is sufficiently large to overcome the activation energy of diffusion one can expect the diffusion of Si into the hexaferrite. Si was speculated to cause the transformation from *M*-type to *W*-type ferrite.<sup>7</sup> Chemical depth profiling is underway to measure the degree of Si diffusion into the ferrite lattice. Earlier studies<sup>8</sup> have in fact measured the propensity of Si to diffuse from the SiC to the ferrite. The substrate preparation conditions also play an important role in this transformation. From the evidence provided it appears that the transformation is more complete in those films prepared using a dry etched SiC. This may be due to the creation of a more pristine surface for the ferrite to grow and thus provide an improved interface for diffusion. It is encouraging that samples studied in which buffer layers were used at the film-substrate interface do not show signs of degradation, diffusion, or structural and magnetic changes.

## ACKNOWLEDGMENTS

This research was supported by the Office of Naval Research and the Defense Advanced Research Program Agency.

<sup>1</sup>I. Zaquine, H. Benazizi, and J. C. Mage, *J. Appl. Phys.* **64**, 5822 (1988); V. G. Harris, Z. Chen, Y. Chen, S. D. Yoon, T. Sakai, A. Gieler, A. Yang, Y. He, K. S. Ziemer, N. Sun, and C. Vittoria, *ibid.* **99**, 08M911 (2006).

<sup>2</sup>Z. Chen, A. Yang, S. D. Yoon, K. Ziemer, C. Vittoria, and V. G. Harris, *J. Magn. Magn. Mater.* **301**, 166 (2006).

<sup>3</sup>Z. Chen, A. Yang, Z. Cai, S. D. Yoon, K. Ziemer, C. Vittoria, and V. G. Harris, *IEEE Trans. Magn.* **42**, 2855 (2006).

<sup>4</sup>T. L. Goodrich, J. Parisi, Z. Cai, and K. S. Ziemer, *Appl. Phys. Lett.* **90**, 042910 (2007).

<sup>5</sup>Z. Chen, A. Yang, A. Geiler, V. G. Harris, C. Vittoria, P. R. Ohodnicki, K. Y. Goh, M. E. McHenry, Z. Cai, T. L. Goodrich, and K. Ziemer, *Appl. Phys. Lett.* **91**, 182505 (2007).

<sup>6</sup>Y. Chen, A. L. Geiler, T. Chen, T. Sakai, C. Vittoria, and V. G. Harris, *J. Appl. Phys.* **101**, 09M501 (2007).

<sup>7</sup>S. K. Mandal, K. Singh, and D. Bahadur, *J. Mater. Sci.* **29**, 3738 (1994).

<sup>8</sup>Z. Cai, Z. Chen, T. L. Goodrich, V. G. Harris, and K. S. Ziemer, *J. Cryst. Growth* **307**, 321 (2007).